NASA TECHNICAL TRANSLATION NASA TT F-15, 151

DEFLECTION OF A FREE FLUID JET AT A FLAT PANEL

W. Schach

Translation of "Umlenkung eines freien Flüssigkeitsstrahles an einer ebenen Platte," Ingenieur-Archiv, Vol. 5, 1934, pp. 245-265

NATIONAL AERONAUTICS AND SPACE ADMINISTRATION
WASHINGTON, D.C. 20546 OCTOBER 1973

STANDARD TITLE PAGE

1. Report No. NASA TT F-15,151	2. Government Accession No.	3. Recipient's Catalog No.
4. Title and Subtitle: DEFLECTION OF A FREE FLUID JET AT A FLAT PANEL		5. Report Date: October 1973 6. Performing Organization Code
7. Author(s): W. Schach		8. Performing Organization Report No. 10. Work Unit No.
9. Performing Organization Name and Address: Leo Kanner Associates, Redwood City, California 94063		11. Contract or Grant No. NASw-2481 13. Type of Report and Period Covered: Translation
12. Sponsoring Agency Name and Address: National Aeronautics and Space Administration, Washington, D.C. 20546		14. Sponsoring Agency Code

15. Supplementary Notes

Translation of "Umlenkung eines freien Flüssigkeitsstrahles an einer ebenen Platte," Ingenieur-Archiv, Vol. 5, 1934, pp. 245-265

16. Abstract Prandtl's hodograph method is used to calculate the free jet boundary and distribution of flow within a planar jet and pressure distribution along the panel upon which it impinges. These are used to determine the stagnation line and the distance between stagnation point and center of jet, distribution of water flowing over the panel, jet "pressure" and its point of application. A setup is described with which pressure distribution over the panel, curves for vertical jet pressure, and its point of application are determined experimentally for comparison with theory. Jet pressure is also checked directly by weighing. Agreement is very good. For constant jet thickness over the panel, pressure distribution along the panel and jet pressure vary as the square of jet velocity and linearly as the sine of panel inclination. The pressure distribution over a panel deflecting a circular jet is determined experimentally at the same panel angles as for the planar jet. Stagnation point, stagnation pressure, jet pressure and its point of application are calculated; jet pressure is also determined by weighing. Again, jet pressure is found to vary as the square of velocity and linearly as the sine of inclination.

17. Key Words (Selected by Author(s))	18. Distribution Statement: Unclassified-Unlimited		
19. Security Classif. (of this report): Unclassified	20. Security Classif. (of this page): Unclassified	21. No. of Pages: 37	22. Price

DEFLECTION OF A FREE FLUID JET AT A FLAT PANEL

W. Schach

1. Introduction

/245*

This article discusses the deflection of a free fluid jet at a flat panel positioned perpendicular and oblique to the direction of flow. This problem, which is of general interest and has also been mentioned very frequently in the literature[1], has never yet been treated in detail, either theoretically or experimentally. Reich [3] merely studied the deflection of a circular water jet at a flat panel perpendicular to the direction of flow and determined the form of flow by means of an equation found empirically. This deflection of a free water jet is important in water-turbine construction for characterizing flow in the deflectors of free-jet turbines and as it impinges upon the blades, and can also frequently be found elsewhere, such as in the impingement of the free jet of water discharged from pipelines and orifices, or falling over dams, upon structural components and walls.

The objective of the following article is to determine the shape of the jet in its deflection and the velocity distribution within the jet, as well as to calculate the pressure distribution upon the panel, plus the magnitude and point of application of the total force normal to the panel. The study is extended to jets with rectangular and circular cross sections. For the rectangular jets, the width of the jet will be taken large enough, relative to the thickness of the jet, that the requirement of planar flow is satisfied. For the sake of brevity, the jet of rectangular cross section will be referred to below as a planar jet, that of circular

---

[1] Bibliography for the fluid jet problem, p. 37.

* Numbers in the margin indicate pagination in the foreign text.

cross section, as a round jet. The panel inclinations were selected between 90° and 30° relative to the direction of flow in each case. The axis of the jet is horizontal, and velocity in the jet corresponds to varying pressure heads of 10 to 25 m water.

The planar problem of the rectangular jet can be characterized completely with the aid of Prandtl's hodograph method (see Betz' article [1]). Determination of the jet boundary for the circular jet upon perpendicular impingement on a flat panel by the method of successive approximations, which Trefftz [2] used to calculate the contraction of circular fluid jets, has likewise been solved and is to be published in a later article. The present article is restricted, in the case of the circular jet, to a theoretical and experimental study of the distribution of the flow of water, the distribution of pressure over the panel, and the determination of overall jet pressure at various angles of inclination.

The experiments were carried out in the Institut für Wasserkraftmaschinen at the Technische Hochschule Hannover [12]; water was selected as the flow medium.

II. Theoretical Treatment of the Deflection of a Planar Water Jet at a Flat Panel /246

1. Deflection of a Planar Water Jet at a Flat Panel Perpendicular to the Direction of Flow.

a) Prandtl's Hodograph Method

In the following study, the deflection of a rectangular jet will be considered as planar potential flow, neglecting gravity. Prandtl's hodograph method [1] is used for the theoretical treatment. If $\Omega = \phi + i\psi$ is the complex potential of a planar flow, then the hodograph method consists of determining the conformal projection of the plane of flow $z = x + iy$ upon a w-plane using

$$w = \frac{d\Omega}{dz} \qquad (1)$$

and thus

$$w = u - iv$$

is simply conjugate-complex velocity. From (1) we obtain

$$z = \int \frac{1}{w} \frac{d\Omega}{dw} dw. \qquad (2)$$

b) Representation of the Hodograph for Deflection of the Planar Jet /247

In the z-plane, we lay the panel on the x-axis and the center of the jet on the y-axis, so that the stagnation point falls at the origin of the rectangular coordinate system; Fig. 1 then shows flow behavior in the z-plane. In the hodograph (w-plane) (Fig. 2) we obtain a source-sink flow in a space delimited by a semicircle and a diameter. The source is located at point A at a distance v_1 along the positive v-axis, while points B and B' are mapped on the positive and negative u-axes, respectively, as sinks at distance v_1. The segment BB' on the u-axis indicates the panel, and interval AO on the v-axis, the center of the jet. Jet branches ACB and AC'B' are mapped in the two circular arcs ACB and AC'B'. All the other flow lines begin at source A and end at sources B and B'. Since no discontinuous velocity changes occur in the plane of flow, the flow lines likewise continuously fill out the region available to them.

c) The Function $\Omega(w)$

In order to make the u-axis a fixed boundary, it is necessary to assign to the source and sinks a corresponding source and sinks of equal capacity, as a mirror image. Mirroring the interior of the circle at the circle's perimenter transforms the full circle into the infinitely extended plane. The capacities of these sources and sinks are doubled in the process. If we set the width a of the

jet at infinity equal to 1, taking $v_1 = 1$ as velocity at infinity, the boundary circle of the w-plane is transformed into the unit circle; the sources are located at +i and -i, the sinks at +1 and -1, and their capacity is C = 2.

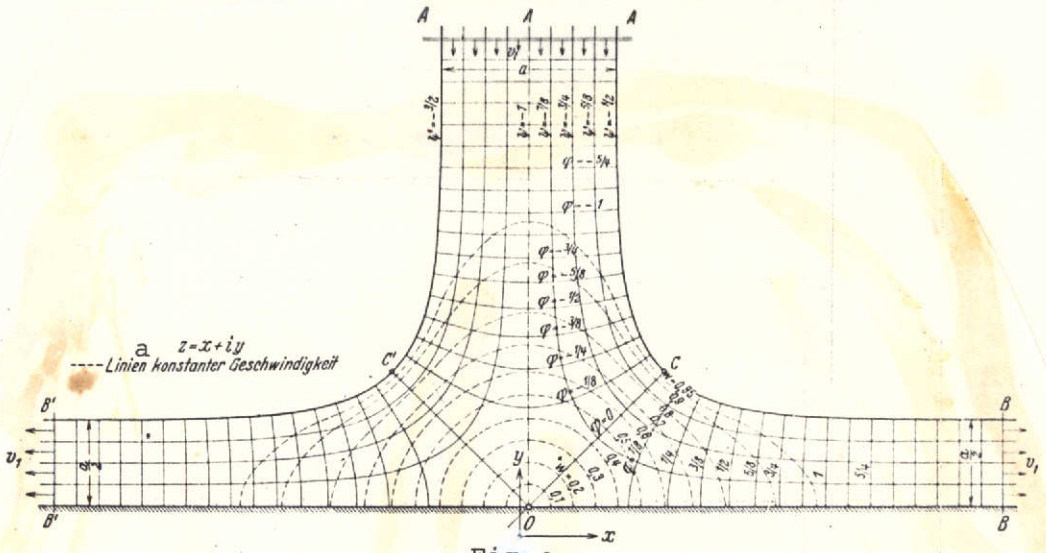

Fig. 1.

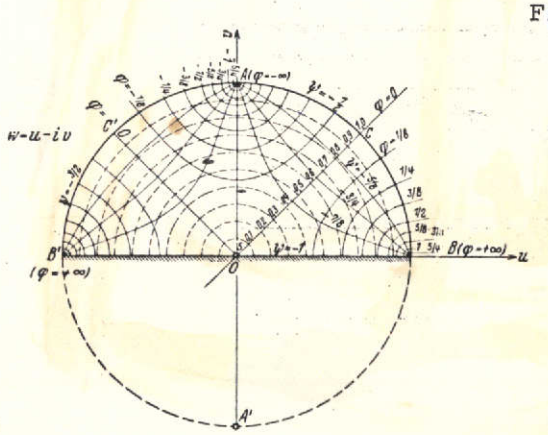

Fig. 2.

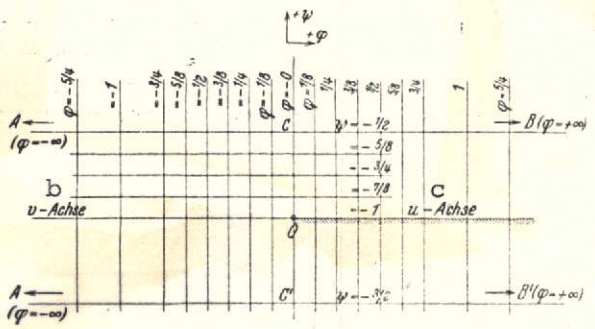

Fig. 3.

Figs. 1 through 3. Representation of the plane of flow, the hodograph and the (ϕ,ψ)-plane for $\alpha_0 = 90°$.

Key: a. Lines of constant velocity
b. v-axis
c. u-axis

[Translator's note: commas in numerals are equivalent to decimal points.]

The field of a planar point source or sink at point w_0 is represented by an analytical function

$$\Omega(w) = \pm \frac{E}{2\pi} \ln (w - w_0) ,$$

where the plus-sign represents the source, and the minus-sign represents the sink. For the flow under study we thus obtain the following potential function

$$\Omega(w) = \frac{1}{\pi} [\ln (w-i) + \ln (w+i) - \ln (w-1) - \ln (w+1)] \qquad (3)$$

or, summarized,

$$\Omega(w) = \frac{1}{\pi} \ln \frac{w^2+1}{w^2-1} . \qquad (3a)$$

In order to plot the network of flow and potential lines in the w-plane, the function $\Omega(w)$ is conformally mapped on a (ϕ,ψ)-plane (Fig. 3) in such a manner that the flow lines ψ = const and the potential lines ϕ = const of the w-plane are transformed into straight lines in the (ϕ,ψ)-plane, parallel to the axis. Reflection of (3a) yields

$$w^2 = \frac{e^{\pi\Omega}+1}{e^{\pi\Omega}-1} = i \operatorname{ctg} \frac{i\pi\Omega}{2} . \qquad (4)$$

d) The Equation of Flow in the z-Plane

If we obtain $\frac{d\Omega(w)}{dw}$ from (3) and integrate in accordance with (2), we obtain

$$z = \frac{1}{\pi} \left[\int \frac{dw}{w(w-i)} + \int \frac{dw}{w(w+i)} - \int \frac{dw}{w(w-1)} - \int \frac{dw}{w(w+1)} \right]$$

or

$$z = \frac{1}{\pi} \left[\ln \frac{w+1}{w-1} + i \ln \frac{w+i}{w-i} \right] + C . \qquad (5)$$

We calculate the integration constant C from the fact that w = 0 for z = 0, and obtain C = 1 - i. In the equation

$$z = \frac{1}{\pi} \left[\ln \frac{w+1}{w-1} + \pi + i \left(\ln \frac{w+i}{w-i} - \pi \right) \right] \qquad (6)$$

the real part is then the x-coordinate and the imaginary part the y-coordinate of a point z which is assigned to point w. From Eqs. (4) and (6), it is possible to plot the flow pattern in the z-plane with the aid of the (ϕ,ψ)-plane by first calculating the associated w for a particular value $\Omega = \phi + i\psi$ and mapping this point into the z-plane, using Eq. (6). The computation yields a simple result, since the general equations (4) and (5) can be considerably simplified for specific values of w and z, as is shown in Sections e) through g), below. /248

e) The Equation for the Line of Symmetry OC

The Ω values at C and O follow from (4):

At C, $w = \sqrt{i}$, i.e. $\Omega = -i/2$ or $\phi = 0$, $\psi = -1/2$;
At O, $w = 0$, i.e. $\Omega = -i$ or $\phi = 0$, $\psi = -1$.

The line of symmetry OC is thus represented by $\phi = 0$ and from (4), with $\Omega \equiv i\psi$, we obtain

$$w^2 = -i \operatorname{ctg} \frac{\pi \psi}{2}. \qquad (7)$$

In the z-plane, it is not possible to simplify Eq. (6) for the line of symmetry.

f) The Equation for the Free Jet Boundary

The value of the flow function at point C is $\psi = -1/2$. For the circle, $\Omega \equiv \phi - 1/2$, and from (4) we thus obtain

$$w^2 = \frac{e^{\pi\varphi} + i}{e^{\pi\varphi} - i}. \qquad (8)$$

In order to determine the free jet boundary in the z-plane, we set $w = e^{i\alpha}$, where α refers to the angle between the free jet and the u-axis; from (5), then,

$$z = \frac{i}{\pi}\left[\int \frac{d\alpha}{e^{i\alpha} - i} + \int \frac{d\alpha}{e^{i\alpha} + i} - \int \frac{d\alpha}{e^{i\alpha} - 1} - \int \frac{d\alpha}{e^{i\alpha} + 1}\right]$$

or

$$z = \frac{1}{\pi}\left[\ln \operatorname{ctg} \frac{\alpha}{2} + i \operatorname{ctg}\left(\frac{\pi}{4} - \frac{\alpha}{2}\right)\right] + C. \qquad (9)$$

For computation it proves desirable to transform the coordinate system by parallel displacement in such a manner that the origin falls at point C ($\alpha = \pi/4$). Then the integration constant becomes

$$C = -\frac{1}{\pi}\left[\ln \operatorname{ctg} \frac{\pi}{8} + i \operatorname{ctg} \frac{\pi}{8}\right],$$

and the coordinates of a point on the free jet boundary, with C as the origin, have the value

$$x = \frac{1}{\pi}\left[\ln \operatorname{ctg} \frac{\alpha}{2} - \ln \operatorname{ctg} \frac{\pi}{8}\right],$$
$$y = \frac{1}{\pi}\left[\ln \operatorname{ctg}\left(\frac{\pi}{4} - \frac{\alpha}{2}\right) - \ln \operatorname{ctg} \frac{\pi}{8}\right]. \qquad (10)$$

g) The Equation of Points Along the Panel and the Center of the Jet

For origin 0, the value of the flow function is $\psi = -1$. Complex potential is then $\Omega \equiv \phi - i$ along the panel, and from (4) it follows that

$$w^2 = \frac{e^{\pi\varphi} - 1}{e^{\pi\varphi} + 1}. \qquad (11)$$

In polar coordinates, on the other hand, $w = r$ in the w-plane along the panel, and we obtain the abscissa of a point on the panel from (6), relative to origin 0,

$$x = \frac{1}{\pi}\left[\ln\frac{1+r}{1-r} - 2\operatorname{arctg}\frac{1}{r} + \pi\right], \qquad (12)$$

where $0 < r < 1$. With the aid of this equation it is possible to determine the velocity profile, and thus the pressure profile, along the panel, as is shown in Section 2.

The ordinate of a point on the y-axis follows immediately from /249 Eq. (12), since the coordinates must correspond, due to the symmetry of the jet; then

$$y = \frac{1}{\pi}\left[\ln\frac{1+r}{1-r} - 2\operatorname{arctg}\frac{1}{r} + \pi\right]. \qquad (13)$$

Simplified equations (7) through (13) can be used to determine the points of equal potential at the center of the jet, at the panel and at the free jet boundary. In contrast, the flow lines within the jet must be calculated from the general equations.

2. Deflection of a Planar Water Jet at a Flat Panel Oblique to the Direction of Flow

a) Mapping the Flow in the Hodograph

If the jet impinges upon the panel obliquely at an angle of α_0, different quantities of water flow to each side.

If we designate the quantity of water flowing upward as q_1, that flowing downward as q_2, while the total quantity of water is q, then q_1 and q_2 are calculated -- by equating the momenta in the direction of the panel -- as follows:

$$\frac{q_1}{q_2} = \frac{1+\cos\alpha_0}{1-\cos\alpha_0}, \qquad (14)$$

and, from the equation of continuity, we have

$$q_1 + q_2 = q. \qquad (15)$$

We place the origin of our rectangular coordinate system at stagnation point 0, with the panel coinciding with the x-axis. From this we obtain the flow behavior shown in Fig. 4 for $\alpha_0 = 45°$. In the hodograph (Fig. 5) we obtain one source at point A ($e^{i\alpha_0}$) and two sinks at B (+1) and B' (-1). The angle AOB = α_0 in the /250
hodograph corresponds to the angle (180 - α_0) in the z-plane, and circular arc AB represents jet branch ACB, while jet branch AC'B' is mapped in arc AB'. The origin of the w-plane coincides with the origin of the z-plane; connecting line AO yield the stagnation line.

b) The Function $\Omega(w)$

If we pursue the same considerations as above, we obtain the following sources and sinks for $v_1 = 1$ and $a = 1$:

Source at A ($e^{i\alpha_0}$) with a capacity of 2,
Source " A' ($e^{-i\alpha_0}$) " " " " 2,
Sink " B (+1) " " " " $2(1 + \cos\alpha_0)$
Sink " B' (-1) " " " " $2(1 - \cos\alpha_0)$

For an arbitrary point, the potential function then reads

$$\Omega(w) = \frac{1}{\pi}\left[\ln(w - e^{i\alpha_0}) + \ln(w - e^{-i\alpha_0}) - (1 + \cos\alpha_0)\ln(w - 1) - (1 - \cos\alpha_0)\ln(w + 1)\right] \quad (16)$$

or, collecting like terms

$$\Omega(w) = \frac{1}{\pi}\left[\ln\frac{w^2 - 2w\cos\alpha_0 + 1}{w^2 - 1} + \cos\alpha_0 \ln\frac{w+1}{w-1}\right]. \quad (16a)$$

c) Representation of Source-Sink Flow in the Hodograph by Means of Flow and Potential Lines

In the conformal mapping of the w-plane onto the (ϕ,ψ)-plane, the problem exists that w cannot be expressed interms of Ω. Thus in order to be able to determine flow lines of equal quantities of water and equipotential lines in the w-plane, it is necessary to proceed as follows: In the w-plane, the points of which are given

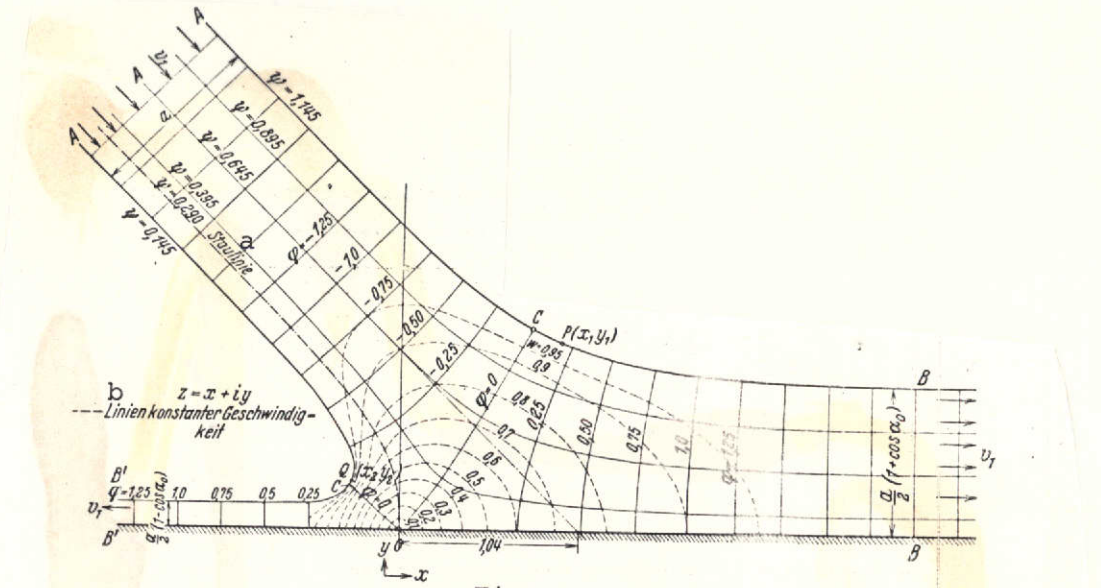

Fig. 4.

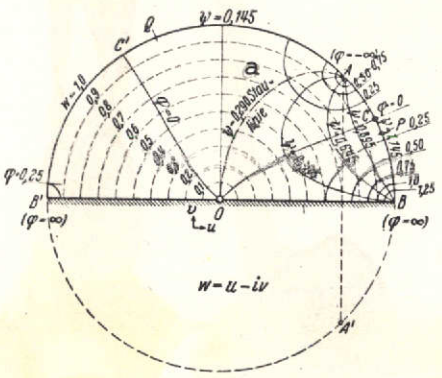

Fig. 5.

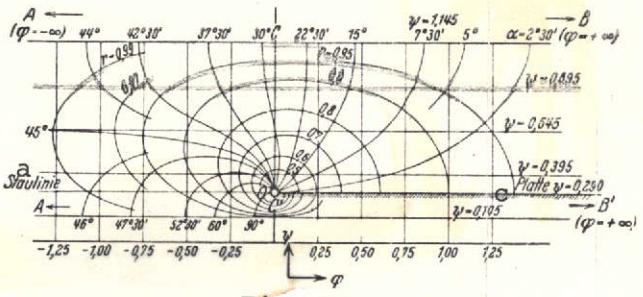

Fig. 5.

Fig. 4 through 6. Representation of the plane of flow, the hodograph and the (ϕ,ψ) plane for $\alpha_o = 45°$.

Key: a. Stagnation line
b. Lines of constant velocity
c. Panel

in polar coordinates by $w = re^{i\alpha}$, lines r = const (concentric circles about the origin) and lines α = const (rays emanating from the origin) are plotted for specific values of r and α. For each point w determined by the intersection of curves r = const and α = const, we can ascertain the associated ϕ and ψ by breaking up the potential function (16) into its real and imaginary parts. If these points are mapped into the (ϕ,ψ)-plane, the resulting series

of lines represent the conformal mapping of curves r = const and α = const (Fig. 6). If we now plot flow lines ψ = const and corresponding potential lines ϕ = const (square scale system), the associated r- and α-values can be determined by interpolation and transferred back into the w-plane, whereby the flow line pattern is determined in the latter.

d) The General Equation of Flow in the z-Plane

In order to derive the general equation of flow, we formulate $\frac{d\Omega(w)}{dw}$ from (16) and integrate in accordance with (2). We obtain

$$z=\frac{1}{\pi}\left[\int\frac{dw}{w(w-e^{i\alpha_0})}+\int\frac{dw}{w(w-e^{-i\alpha_0})}-(1+\cos\alpha_0)\int\frac{dw}{w(w-1)}-(1-\cos\alpha_0)\int\frac{dw}{w(w-1)}\right]$$

or

$$z=\frac{1}{\pi}\left[\frac{1}{e^{i\alpha_0}}\ln(w-e^{i\alpha_0})+\frac{1}{e^{-i\alpha_0}}\ln(w-e^{-i\alpha_0})+\ln\frac{w+1}{w-1}-\cos\alpha_0\ln(w^2-1)\right]+C.$$

We determine the integration constant C for w = 0 to be

$$C=-\frac{1}{\pi}[2\alpha_0\sin\alpha_0+i\pi(1+\cos\alpha_0)];$$

the general equation of flow then reads

$$z=\frac{1}{\pi}\left[\frac{1}{e^{i\alpha_0}}\ln(w-e^{i\alpha_0})+\frac{1}{e^{-i\alpha_0}}\ln(w-e^{-i\alpha_0})+\ln\frac{w+1}{w-1}-\cos\alpha_0\ln(w^2-1)-2\alpha_0\sin\alpha_0-i\pi(1+\cos\alpha_0)\right]. \quad (17)$$

e) The Equation of the Free Jet Boundary

/251

Points on the circle in the w-plane have the form $w = e^{i\alpha}$ in polar coordinates; we thus obtain

$$z=\frac{i}{\pi}\left[\int\frac{d\alpha}{e^{i\alpha}-e^{i\alpha_0}}+\int\frac{d\alpha}{e^{i\alpha}-e^{-i\alpha_0}}-(1+\cos\alpha_0)\int\frac{d\alpha}{e^{i\alpha}-1}-(1-\cos\alpha_0)\int\frac{d\alpha}{e^{i\alpha}+1}\right]$$

or

$$z=\frac{1}{\pi}\left[\cos\alpha_0\ln\frac{\cos\alpha_0-\cos\alpha}{2\sin\alpha}+\ln\operatorname{ctg}\frac{\alpha}{2}+\frac{i\sin\alpha_0}{2}\ln\frac{1-\cos(\alpha+\alpha_0)}{1-\cos(\alpha-\alpha_0)}\right]+C. \quad (18)$$

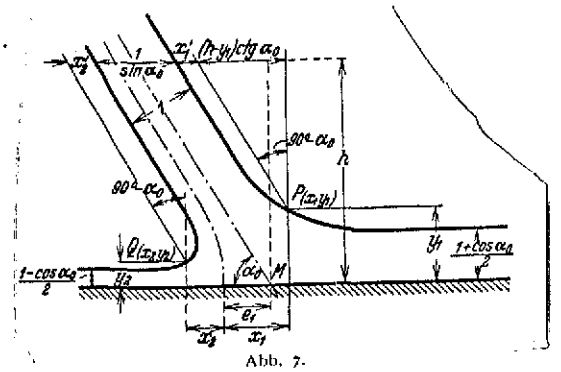

Fig. 7. Determination of the distance of the stagnation point from the center of the jet.

To determine the free jet boundaries, we first calculate two points P and Q of the free jet (Fig. 7) from general flow equation (17). We shift the origin of the rectangular coordinate system to these points. The constant C is then determined for $\alpha = \alpha_P$ and for $\alpha = \alpha_Q$ from the condition $z = 0$, and we can thus calculate the coordinates of the free jet boundaries relative to P and Q.

f) The Equation of Points Along the Panel

For the points along the panel, the general equation of flow in the z-plane takes the following form, with $w = r$:

$$z = \frac{1}{\pi}\left[\frac{1}{e^{i\alpha_0}}\ln(r - e^{i\alpha_0}) + \frac{1}{e^{-i\alpha_0}}\ln(r - e^{-i\alpha_0}) + \ln\frac{r+1}{r-1} - \cos\alpha_0 \ln(r^2 - 1)\right] + C.$$

We break up the individual terms into their real and imaginary parts and obtain the abscissa of a point x on the panel, calculated from origin O,

$$x = \frac{1}{\pi}\left[\cos\alpha_0 \ln\frac{r^2 + 1 - 2r\cos\alpha_0}{1 - r^2} - 2\sin\alpha_0 \arccos\frac{r - \cos\alpha_0}{\sqrt{r^2 + 1 - 2r\cos\alpha_0}} + \right.$$
$$\left. + \ln\frac{1+r}{1-r} + 2\sin\alpha_0(\pi - \alpha_0)\right], \qquad (19)$$

where r runs from -1 to +1.

g) Distance of the Stagnation Point from the Center of the Jet

Yet another equation will be derived below, by means of which the distance e_1 of the stagnation point from the center of the jet can be calculated without knowing the external shape of the

jet. From Fig. 7 we have

$$e_1 = x_1 + y_1 \operatorname{ctg} \alpha_0 - x_1' - \frac{1}{2 \sin \alpha_0}. \qquad (20)$$

In order to be able to determine e_1 from this equation, we assume point P on the jet boundary for which the conjugate velocity vector has the value $w = e^{i\alpha_0/2}$. In this case, it is possible to simplify Eq. (17), and we obtain the following values for x_1 and y_1:

$$x_1 = \frac{1}{\pi}\left[\cos\alpha_0 \ln \frac{\sin\frac{3\alpha_0}{4}}{\cos\frac{\alpha_0}{4}} + \ln \operatorname{ctg}\frac{\alpha_0}{4} + \sin\alpha_0 (\pi - \alpha_0)\right],$$
$$y_1 = \frac{1}{\pi}\left[\sin\alpha_0 \ln \frac{\sin\frac{3\alpha_0}{4}}{\sin\frac{\alpha_0}{4}} + \frac{\pi}{2}(1 + \cos\alpha_0)\right]. \qquad (21)$$

We calculate the absolute value of x'_1 by transformation of the coordinate system into the x'y-direction from (18), obtaining

$$|x_1'| = -\frac{1}{\pi}\left[\cos\alpha_0 \ln \sin\alpha_0 + \ln \operatorname{ctg}\frac{\alpha_0}{2} - \cos\alpha_0 \ln \frac{\sin\frac{3\alpha_0}{4}}{2\cos\frac{\alpha_0}{4}} - \right.$$
$$\left. - \ln \operatorname{ctg}\frac{\alpha_0}{4} - \cos\alpha_0 \ln \frac{\sin\frac{3\alpha_0}{4}}{\sin\frac{\alpha_0}{4}}\right]. \qquad (22)$$

/252

On the basis of the calculations from the jet equation, the value of x'_1 becomes negative, due to the choice of coordinate system, and must be given a negative sign, since only the absolute value of x'_1 comes under consideration for Eq. (20). If we substitute the values of x_1, y_1 and x'_1 from Eqs. (21) and (22) into Eq. (20), we obtain

$$e_1 = \frac{1}{\pi}\left[\cos\alpha_0 \ln \sin\alpha_0 + \ln \operatorname{ctg}\alpha_0 + 0{,}693 \cos\alpha_0 + \frac{\pi}{2}(\operatorname{ctg}\alpha_0 + \sin\alpha_0) - \alpha_0 \sin\alpha_0\right]. \qquad (23)$$

3. Jet Pressure and Its Point of Application

With the notation specified above, jet pressure on the panel (Fig. 8) is

$$P_0 = \frac{q\gamma}{g} v_1 \sin\alpha_0. \qquad (24)$$

The condition of equilibrium for momenta in the direction of the panel yields the following relations between a_1, a_2 and a:

$$\left.\begin{aligned} a_1 &= a\frac{1+\cos\alpha_0}{2}, \\ a_2 &= a\frac{1-\cos\alpha_0}{2}, \end{aligned}\right\} a_1 + a_2 = a. \qquad (25)$$

By using the intersection M of the midline of the jet with the panel as a reference point we obtain the distance of the point of application of jet pressure from the jet midline,

$$e = \frac{a}{2}\operatorname{ctg}\alpha_0. \qquad (26)$$

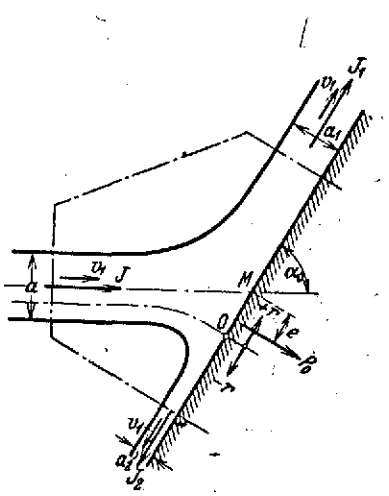

Fig. 8. Determination of jet pressure and its point of application.

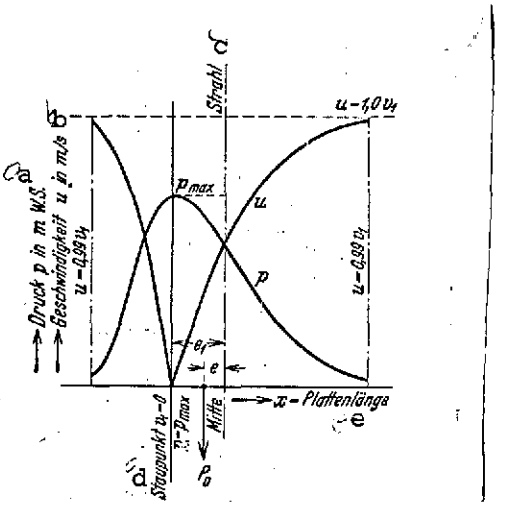

Fig. 9. Theoretical pressure and velocity curves on the panel at $\alpha_0 = 60°$.
Key: a. Pressure p in meters of water; b. Velocity u in m/s; c. Center of jet; d. Stagnation point; e. Length of panel

We determined the velocity distribution along the panel from (19) and, for the special case of perpendicular impingement, from (12). In these equations, r is the ratio of velocity u at the panel to jet velocity v_1 ($0 < u/v_1 < 1$ for the upper jet load, $0 > u/v_1 > -1$ for the lower jet load). For numerical evaluation, we assume certain values u/v_1 and calculate the associated abscissa x. If the configuration of the velocity curve is known, we then obtain the corresponding pressure curve on the basis of Bernoulli's equation,

$$p = \frac{\gamma}{2g} v_1^2 (1 - r^2) \qquad (27)$$

/253

The two curves are shown in Fig. 9 for the angle $\alpha_0 = 60°$.

4. Numerical Examples

Configurations of flow lines within the jet have been determined with the aid of the extended equations for perpendicular flow and for a panel inclination of $\alpha_0 = 45°$. Figs. 1 through 3 and 5 through 7 show the results of computation. In addition, the jet boundaries have been calculated with Eq. (18) for various panel inclinations and compiled in Fig. 10. This figure contains all characteristic values of the flow -- stagnation line, stagnation point, jet pressure and its point of application -- for a jet thickness a = 1 and a velocity $v_1 = 1$. The stagnation line cannot be calculated directly at this point, but for calculating it we do know its location in the impinging jet, and also its "perpendicular tangent" on the panel at the stagnation point. Since the stagnation line experiences sharp curvature as it approaches and becomes the "perpendicular tangent," these values are adequate for plotting it in the flow pattern.

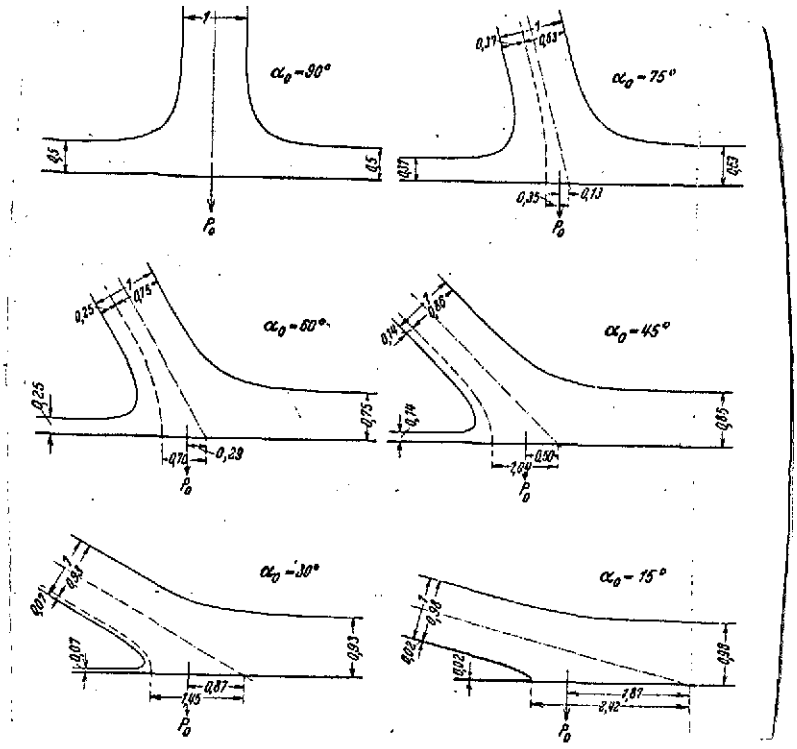

Fig. 10. Theoretical jet configurations at various panel inclinations.

III. Theoretical Treatment of the Deflection of a Circular Water Jet at a Flat Panel

It is possible to determine the external shape of the jet and pressure distribution on the panel with the aid of Trefftz's method [2] for the deflection of a water jet of circular cross section which impinges perpendicularly on a flat panel if we consider the problem in the form of rotationally symmetrical potential flow. A mathematical derivation has not yet been successful for the obliquely impinging jet. We therefore restrict ourselves to computing the quantities of water flowing to both sides. Even though these studies only have qualitative value, they will still be covered briefly because of good agreement with experimental results.

1. Calculation of the Quantities of Water Flowing Off to Both Sides and the Thickness of the Off-flowing Jet

Fig. 11 shows schematically the deflection of a round jet at a flat panel oblique to the direction of flow. A cylinder having the stagnation line as its axis and elements perpendicular to the plane of symmetry divides the water into two parts of different size, which will be determined by the law of the conservation of momentum. For this purpose, we construct a cylinder-like control surface about the jet, as shown in Fig. 11. We choose the radius /254

of the control surface's base on the panel of such a magnitude that the velocity of the jet flowing off is again v_1; experimental results require $R \geq 3.2r$. We also assume that the flow lines extend radially from the stagnation point; according to the experiments conducted with paint, this assumption is valid with sufficient accuracy. If we consider a wedge of water dq_1 or dq_2 in cross section II with central angle $d\phi$, we find the elementary quantities of water, from total quantity of water $Q = r^2\pi v_1$, to be

$$\left.\begin{aligned} dq_1 &= \left(\frac{r_1}{r}\right)^2 \frac{d\varphi}{2\pi} Q, \\ dq_2 &= \left(\frac{r_2}{r}\right)^2 \frac{d\varphi}{2\pi} Q, \end{aligned}\right\} \tag{28}$$

where r_1/r and r_2/r are determined from Fig. 11 by the law of cosines. Since the panel forms an angle of $(90 - \alpha_0)$ with the plane perpendicular to the axis of the jet, the angle ϕ at which the wedge of water under consideration lies in plane II changes to an angle ψ for the plane of the panel, the size of which follows from

$$\tan\psi = \tan\phi \sin\alpha_0 \tag{29}$$

The condition of equilibrium for momenta in the direction of the panel is

$$Q\cos\alpha_0 - \int_0^{Q_1} \cos\psi\, dq_1 + \int_0^{Q_2} \cos\psi\, dq_2 = 0. \tag{30}$$

If we substitute the values of dq_1, dq_2 and ψ from Eqs. (28) and (29), we obtain

$$\frac{\pi\cos\alpha_0}{2\frac{b}{r}} = \int_{-\frac{\pi}{2}}^{+\frac{\pi}{2}} \frac{\cos^2\varphi \sqrt{1 - \frac{b^2}{r^2}\sin^2\varphi}}{\sqrt{1 - \cos^2\alpha_0 \sin^2\varphi}}\, d\varphi. \tag{31}$$

Since b/r is a function only of α_0, while independent of ϕ, integral equation (31) is satisfied if we set

$$b/r = \cos\alpha_0 \qquad (32)$$

If we label the quantity of water flowing off upward as Q_1, the quantity flowing off downward as Q_2 and the total quantity of water as $Q = Q_1 + Q_2$, we can calculate Q_1 and Q_2 from (32), since they correspond to the circular segments of central angle $2\alpha_0$; we then obtain /255

$$\left.\begin{aligned} Q_1 &= Q\left(1 - \frac{\alpha_0^\circ}{180} + \frac{\sin 2\alpha_0}{2\pi}\right), \\ Q_2 &= Q\left(\frac{\alpha_0^\circ}{180} - \frac{\sin 2\alpha_0}{2\pi}\right). \end{aligned}\right| \qquad (33)$$

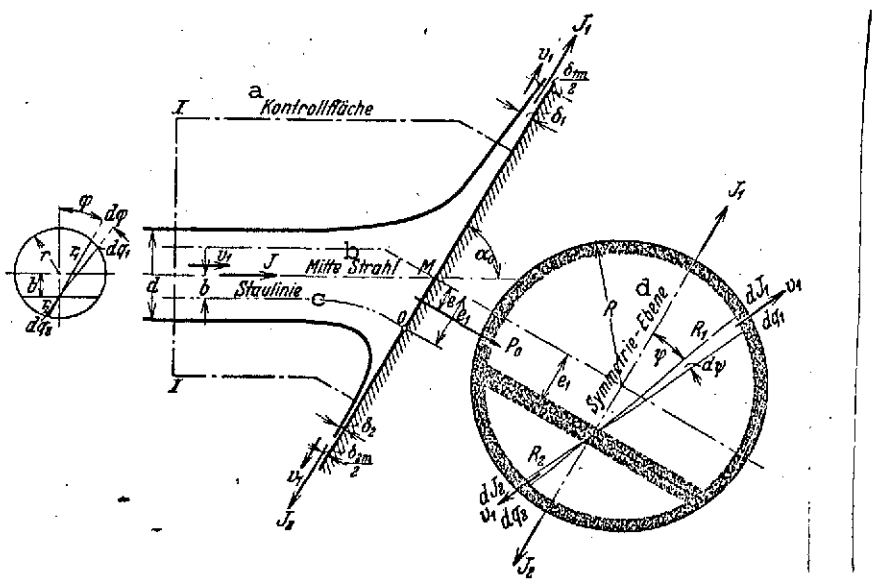

Fig. 11. Deflection of a round jet at a flat panel oblique to the direction of flow.

Key: a. Control surface
b. Center of jet
c. Stagnation line
d. Plane of symmetry.

If we formulate expressions for the elementary quantities of water for the jet flowing off and compare them with the values

from Eq. (28), we obtain the following for the thickness δ of the off-flowing jet:

$$\left.\begin{aligned}\delta_1 &= \frac{1}{R_1}\frac{1-\cos^2\alpha_0\sin^2\varphi}{\sin\alpha_0}\frac{r_1^2}{2},\\ \delta_2 &= \frac{1}{R_2}\frac{1-\cos^2\alpha_0\sin^2\varphi}{\sin\alpha_0}\frac{r_2^2}{2}.\end{aligned}\right\} \qquad (34)$$

It should be pointed out here that the values of δ calculated from (34) apply only to that distance from the center of the jet at which deflection of the jet is complete and velocity has again reached the value b_1, i.e. for $R \geq 3.2\ r$. This equation cannot be applied within the region of deflection. Jet thickness δ has been plotted as a function of angle ψ for panel positions $\alpha_0 = 60$ and 30°. The computation yields a different curve shape than on the basis of Wittenbauer's equation [10, 8]; this can be explained by the fact that Wittenbauer assumes the stagnation point to coincide with the center of the jet, an assumption which does not agree with experiment.

2. Determination of Jet Pressure and Its Point of Application

According to the law of the conservation of momentum, jet pressure perpendicular to the panel [7] is

$$P_0 = \frac{Q\gamma}{g} v_1 \sin\alpha_0. \qquad (35)$$

Setting up the equation of moment about stagnation point O, from Fig. 11, yields

$$P_0(e_1 - e) = J e_1 \sin\alpha_0 - J_1\frac{\delta_{1m}}{2} + J_2\frac{\delta_{2m}}{2}.$$

If we determine "moment arms" $\delta_{1m}/2$ and $\delta_{2m}/2$ as mean values from the moment arms of the elementary momenta, we obtain the following equation for e at r = 1:

$$e = \frac{1}{\pi \sin \alpha_0} \left[\int_0^{\pi/2} R_1 \delta_1^2 \cos \psi \, d\psi - \int_0^{\pi/2} R_2 \delta_2^2 \cos \psi \, d\psi \right]. \qquad (36)$$

As $R \to \infty$, $\delta \to 0$. In order to obtain finite values for e, however, the calculation has been carried out with R = 3.2 r. But this calculation yields no satisfactory agreement with the experimental values which were taken from the measurement of pressure.

IV. The Experimental Setup

1. Description of Test Stand, Nozzles and Test Panel

The bucket turbine connected to the medium-pressure circuit in the water-power machinery lab, Technische Hochschule, Hannover, with a head of about 30 m, was used as the test stand after suitable modification [12]. Figs. 12 and 13 show a diagram of the test set-up, with water circuit, plus an elevation and plan of the modified test system.

It was assumed, for the formulae for the planar jet, that it is infinitely wide, perpendicular to the plane under consideration, and that the same state of flow prevails in all mutually parallel planes. In reality, however, a jet discharging from a rectangular /257 nozzle diverges spatially after impinging upon a flat panel. In the central section of the jet, though, the outflowing "filaments" of water remain in the plane of the impinging filaments and of the perpendiculars to the width of the jet, if the jet's width is sufficiently large, so the requirements of planar flow processes are satisifed. The nozzle was designed with dimensions of 21 × 115 mm at the outlet on the basis of these considerations. The nozzle of the bucket turbine, with needle-valve regulation was used for experiments with a round jet.

The test panel -- a forged-iron 610 × 250 mm plate -- is mounted, free to rotate, in an iron U-frame which is fastened to the housing of the bucket turbine. A hole with a diameter of 180 mm has been cut in the center of it. The connecting piece inserted into this

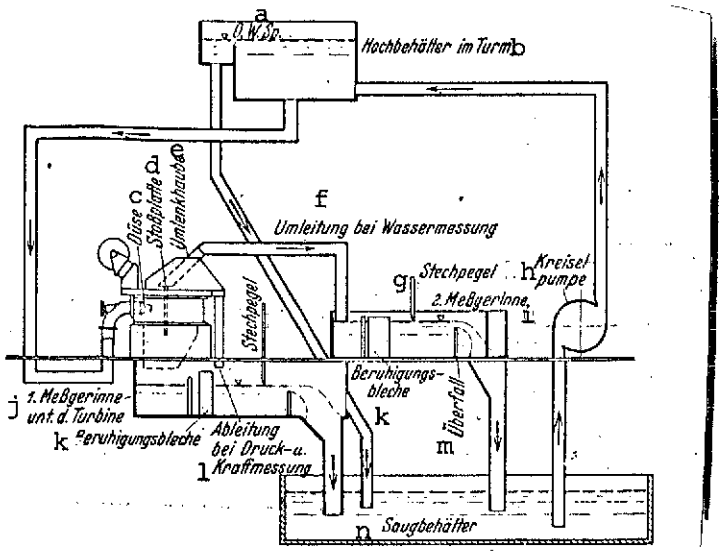

Fig. 12. Schematic diagram of the test setup, with water circuit.

Key: a. O.W.Sp. [Expansion unknown]; b. Elevated tank and tower; c. Nozzle; d. Baffle; e. Deflection hood; f. Bypass during water measurement; g. Insertion gauge; h. Centrifugal pump; i. Second measuring channel; j. First measuring channel under turbine; k. Damping plates; l. Outlet during pressure and force measurement; m. Overflow; n. Aspiration tank.

opening is changed as required by the type of measurements, while the forged-iron panel serves merely to lead the water off properly. The center of the pierced panel will be called "center of panel" in the following. For pressure measurements on the panel, the holes for taking measurements are arranged over a total distance of 160 mm along a diameter of the 180-mm brass disk used as the connecting piece (Fig. 14); the distance between measurement holes is 5 mm. The holes themselves have a diameter of 1 mm and a depth of 3 mm; they lead into little brass tubes, over which the rubber hoses are drawn. In the trials with the planar jet, this measurement line is oriented perpendicular to the plane of the nozzle, whereas for trials with a round jet, it is possible to make measurements in all planes by rotating the brass disk. When force measurements were made by weighing, this brass disk was replaced with a rectangular panel, 90 × 41.5 mm, for the planar jet and with a disk 125 mm in diameter for the round jet. These panels are set up in the forged-iron panel so as to be movable with a play of about 1/5 to 1/10 mm, after the insertion of an adaptor ring, and have a lever on the backside which is mounted below on the main panel, in ball bearings (Fig. 13). There is a cylinder at the upper end of the lever, to which a wire is fastened;

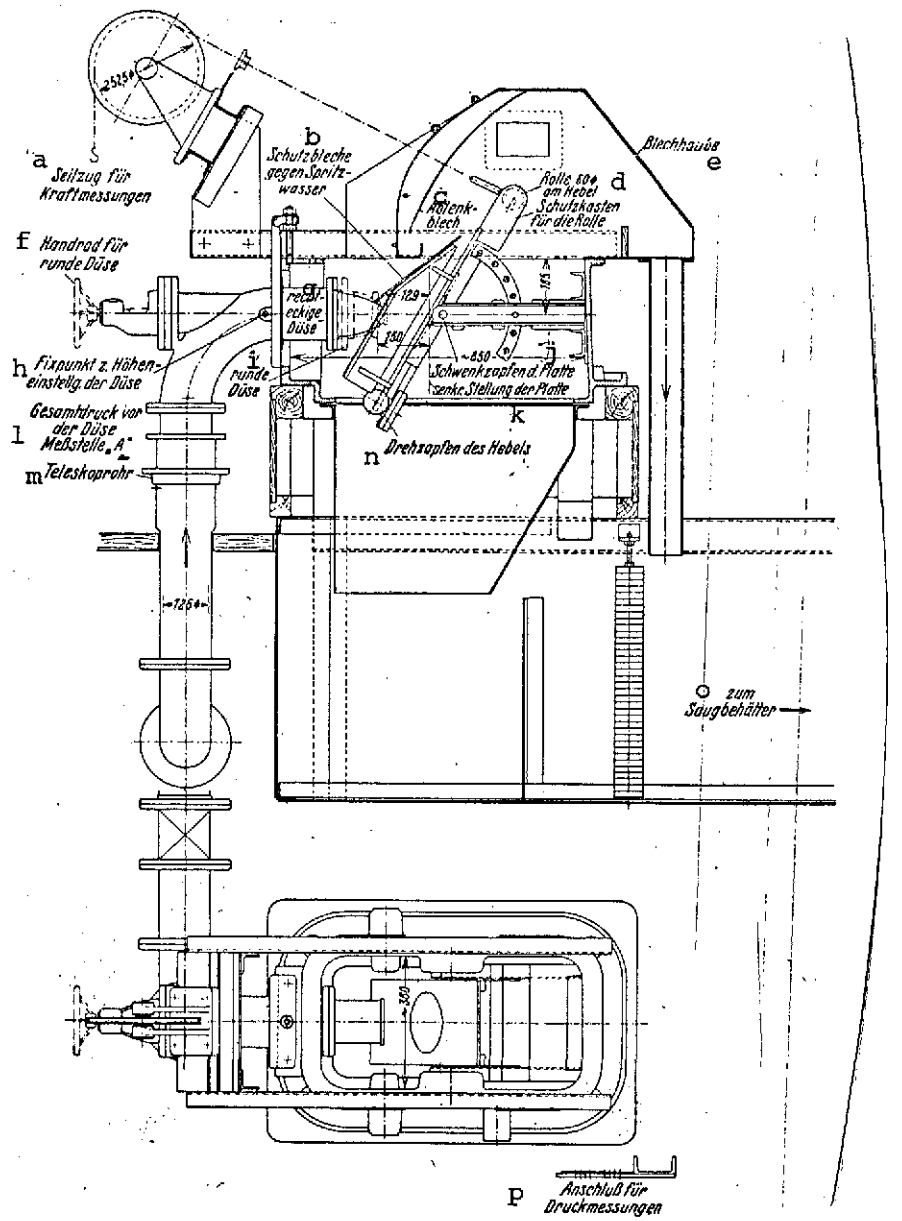

Fig. 13. Design of the test system for pressure and force measurements with planar and round jets.

Key: a. Cable system for force measurements; b. Panels for protection against spatter; c. Deflection panel; d. Cylinder (diameter 60) on lever, protective housing for cylinder; e. Sheet-metal hood; f. Handwheel for round nozzle; g. Rectangular nozzle; h. Fixed point for setting nozzel height; i. Round nozzle; j. Pivot for panel; k. Vertical panel position; l. Total pressure upstream from nozzle, measurement point "A"; m. Telescoping pipe; n. Pivot pin for lever; o. To aspiration tank; p. connection for pressure measurements

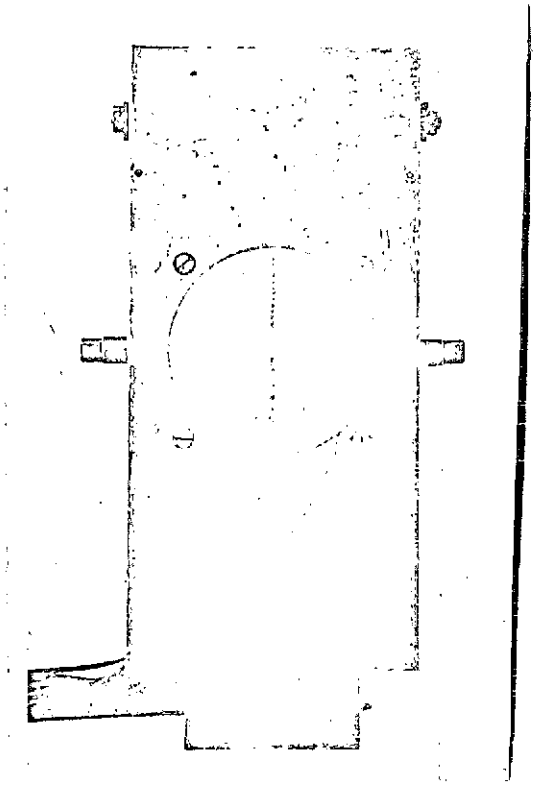

Fig. 14. Configuration of the test panel for pressure measurements.

the latter is led over a pulley in the front section of the housing. A special test panel was designed for water measurement with a round jet, to be fastened on the main panel. This panel is fitted with two cutoff devices in its horizontal center plane, whose points are 155 mm apart, for the purpose of dividing the jet. While the water deflected downward can flow off freely, that flowing upward is guided by a jacket on the panel. At the top, the panel is attached via a connecting piece to a pipeline, which leads to the second measuring channel (Fig. 12).

The test panel is installed in such a manner that the portion of the jet flowing off downward experiences the greatest deflection. Since the nozzle can be shifted by about 60 mm through the insertion of a sort of telescoping tube in the pipeline, the center of the jet could be adjusted relative to the panel in such a manner /258 that the center of the nozzle and that of the panel lay in a horizontal plane. The corresponding nozzle setting was read off at a scale, with vernier, mounted on the side of the housing. An angular spirit level which could be read to 1/20° was used to adjust the panel to the particular angle of inclination.

2. Type of Measurements and Instrumentation

The following were measured:

1. For rectangular and round jets:

a) Pressure distribution at the panel at various panel inclinations and varying jet velocities;

b) Location of the stagnation point on the panel at various panel inclinations;

c) Jet pressure and its point of application:

α) From the measurement of pressure;

β) By weighing;

2. For round jets:

a) The quantities of water flowing off to both sides for various panel settings.

a) Statistical Pressure Measurements

According to studies by Nikuradse [10], measurement holes with a sharp-edged form yield the most accurate results, whereas countersunk holes produce an additional pressure effect. In order to study the effect of the size and type of measurement holes, the pressure curve for the round jet in the vertical plane through the center of the jet at a panel setting of $\alpha_o = 30°$ was therefore determined over a length of 70 mm in the region of high velocities and thin water layers by shifting the nozzle, using sharp-edged holes with diameters of 0.4, 0.7, 1.0 and 1.5 mm; the pressures were measured with a column of water. The trials yielded different values for static pressure, depending upon the diameter of the measurement holes; 0.4-mm holes produced the smallest values, while we obtained larger values up to a diameter of 1.0 mm, the pressures for 1.5 and 1.0 mm approximately coinciding. These measurements were used to determine, by extrapolation, the pressure distribution which would be obtained with a hole of diameter zero in the wall

(cf. [11]). Accordingly, the sharp-edged holes under consideration exhibit the following errors in % of velocity head:

TABLE 1.

Hole diameter, mm	0,4	0,7	1,0	1,5
Indicating error in %	+0,6	+1,1	+1,8	+1,8

Comparison with slightly countersunk measurement holes of diameter 1 mm showed us that the indicating error for these increased to +2.5% on the average. The experimental values from pressure measurements where therefore reduced to the "zero" hole. Mercury U-tubes were used as measurement instruments for the higher pressures, while pressures below 3 m where determined with a column of water. In order to adequately damp fluctuations at the measurement points, capillary tubes with inside diameters of 1/4 to 1/2 mm were inserted in the measurement lines.

b) Stagnation Point Measurements

Once the approximate position of the stagnation point had been established by the measurement of pressure, the pressure about the measurement point being considered was determined as the difference relative to total pressure upstream from the nozzle by shifting the nozzle, using a column of water. The nozzle position at which the smallest pressure differential is measured indicates the position of the stagnation point, while we obtain the magnitude of stagnation pressure from the measured pressure difference. These measurements were only carried out for the rectangular jet.

c) Determination of Pressure Drop

The pressure drop was measured as total pressure upstream from the nozzle by means of a total-pressure instrument at measurement point A (Fig. 13) and was referred to the center of the nozzle by

subtracting the geodetic elevation. Thus these values also involve frictional losses in the elbow and in the nozzle inlet. However, /259 it is not necessary to take the losses into consideration, since the pressure drop serves only as a reference quantity.

d) Measurement of Water

The quantities of water flowing off to both sides were determined for the round jet by measuring overflow with sharp-edged overflows 200 mm wide with lateral contraction, which were calibrated by tank measurements. Overflow height h_o, fluctuations in which averaged ±1/10 for a given operating state, was measured with an insertion gauge. The nozzles were calibrated by tank measurements performed with the aspiration tank (Fig. 12).

e) Force Measurements

The center of the nozzle was adjusted relative to the panel on the basis of the measured pressure curves in such a manner that pressure equalization occurred at the end of the panel. In addition to total pressure upstream from the nozzle, the tension in cable C was measured, the moment of which maintains equilibrium with that associated with the jet pressure. From this we obtain jet pressure:

$$P = Cc/h.$$

The moment arm c associated with the cable tension was determined photographically. The point of application of jet pressure -- such as found by measuring two different moments -- cannot be determined, since the error in measurement affects the results too markedly for the small jet dimensions. The distance e between the jet pressure point and the center of the jet must be determined either on the basis of theoretical formulae or from the measured pressure curve, from which momentum arm h is known.

f) Trials with Paint

The paint trials were used merely as preliminary tests in order to make flow at the panel visible. White enamel was used for the paint. Several of the large number of paint trials are shown in Figs. 15 through 18 for the rectangular and round jets at various panel inclinations α_o.

V. Evaluation of Trials and Comparison of Experimental Results with Theory

1. Trials with Rectangular Jets

a) Nozzle Calibration

In order to calibrate the nozzle, the highest velocity head of the jet H_o [m] was determined as stagnation pressure, as a function of pressure drop H', at $\alpha_o = 90°$, and the quantity of water per second, Q, was measured. From this we obtain the total quantity of water, $Q = 9.62\sqrt{H_o}$ ℓ/s.

b) Evaluation of Pressure Measurements

Pressure measurements were made for panel positions between 90° and 30° at intervals of 15° for a pressure drop of about 10 m. In order to study the effect of the pressure drop, moreover, pressure measurements were performed at panel positions of 90°, 60° and 30° for drops of about 15, 20, and 25 m. We obtain the position of the stagnation point and the magnitude of stagnation pressure, as well as jet pressure and its point of application, as the results of these trials. For the purpose of comparison with theoretical studies, measured and theoretical pressure curves have been plotted in Fig. 19 for jet thickness 1 and jet velocity 1. It is found from a comparison of pressure measurements for different pressure drops that the pressure distribution and jet pressure vary as

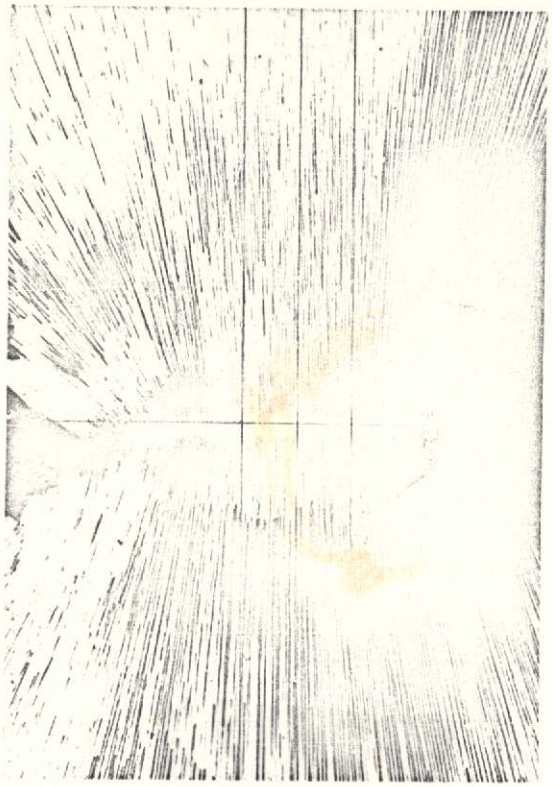

Fig. 15. Rectangular jet, $\alpha_o = 90°$.

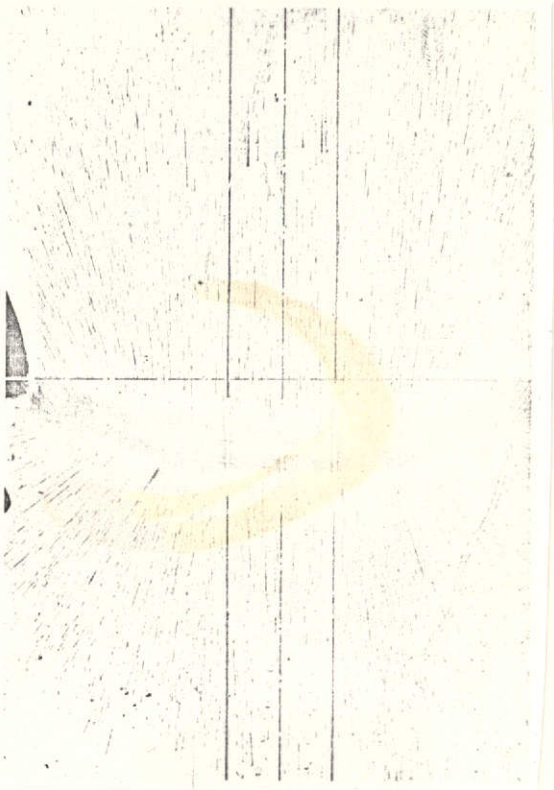

Fig. 16. Rectangular jet, $\alpha_o = 30°$.

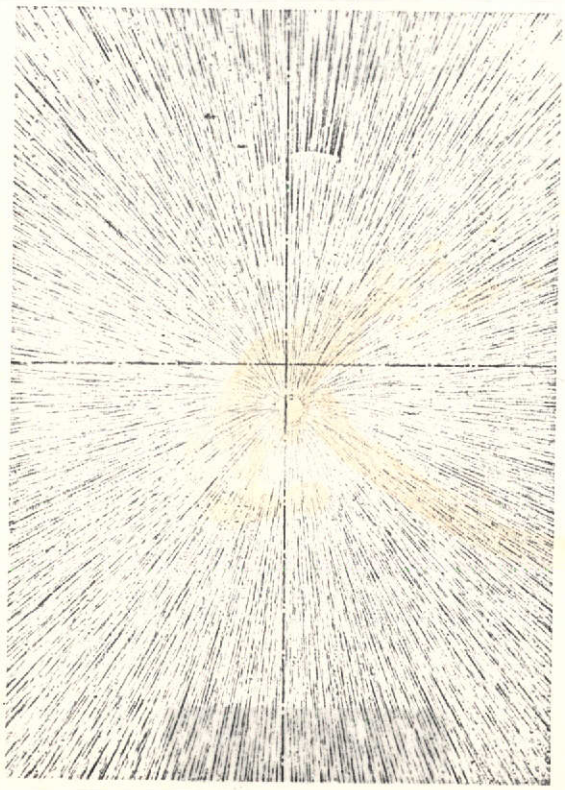

Fig. 17. Round jet, $\alpha_o = 75°$.

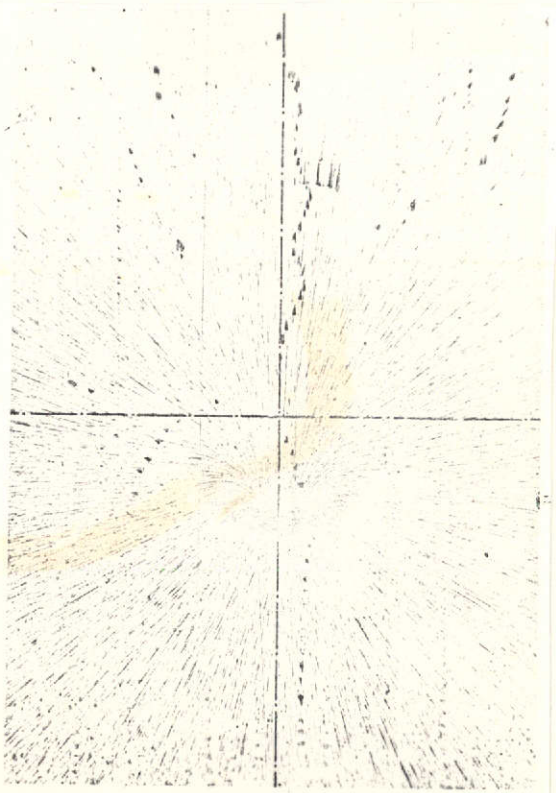

Fig. 18. Round jet, $\alpha_o = 45°$.

the square of velocity for constant jet thickness, i.e. that a dependence upon Reynolds number cannot be found in the range studied. If we represent jet pressure P as a function of maximum stagnation pressure H_o -- measured at $\alpha_o = 90°$ -- it can be balanced for any given angle with a linear function $P = \text{const} \cdot H_o$. As a function of $\sin\alpha_o$, we obtain a value for P of

$$P = 0.350 H_o \sin\alpha_o \text{ [kg]}$$

for a jet width of 1 cm, with a maximum deviation of ±2%. The /261 dimensionless values e/a and e_1/a are also plotted in Fig. 21 as functions of angle α_o, while the curves drawn in represent the theoretical values.

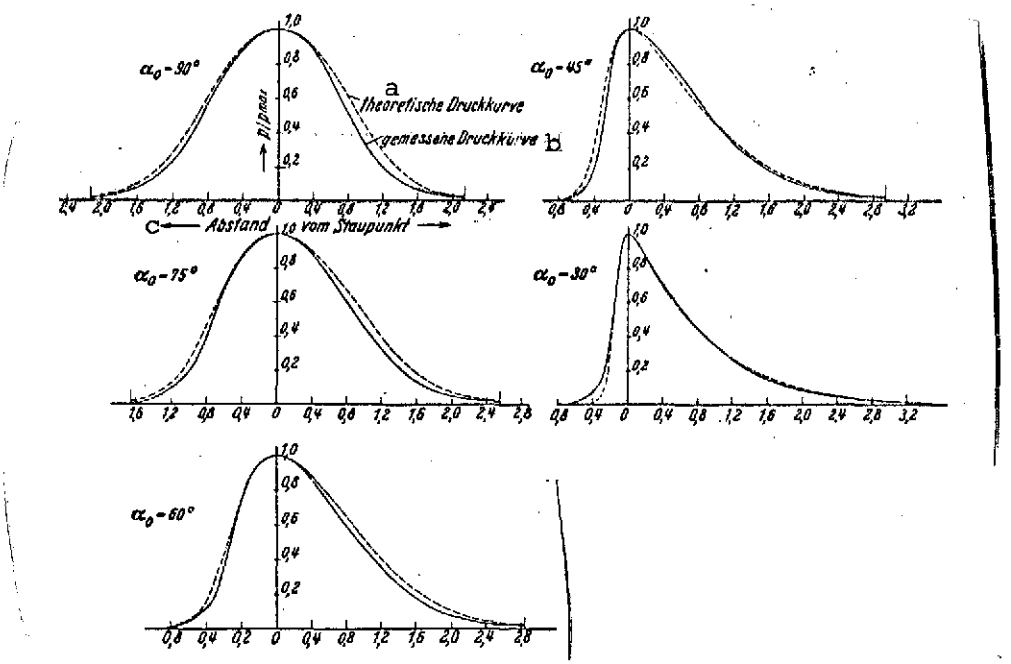

Fig. 19. Comparison of measured and theoretical pressure curves.

Key: a. Theoretical pressure curve
b. Measured pressure curve
c. Distance from stagnation point

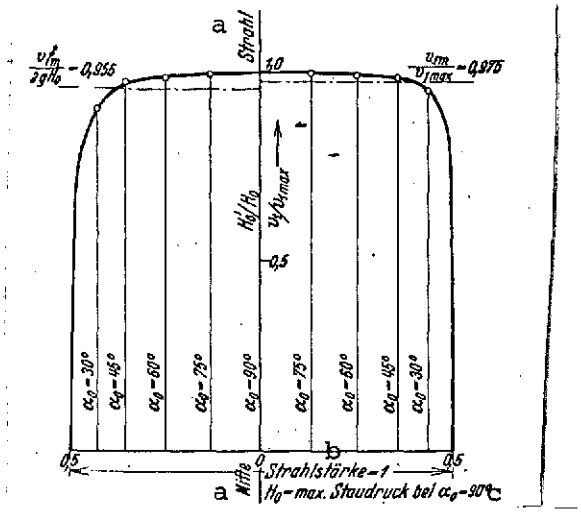

Fig. 20. Determination of mean velocity v_{1m} and mean velocity head $v_{1m}^2/2g$ in the jet.

Key: a. Center of jet; b. Jet thickness; c. max. stagnation pressure at $\alpha_o = 90°$.

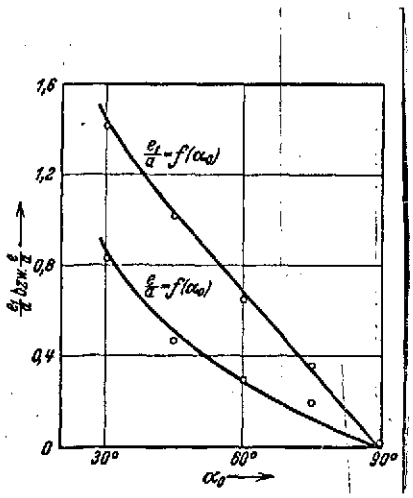

Fig. 21. Distance of stagnation point and point of jet pressure application from center of jet.

Key: bzw. = or

c) Determination of Theoretical Jet Pressure

Velocity at the nozzle outlet was not measured directly, but determined from the stagnation pressures by assuming the locations of the flow filaments on the basis of potential theory. From the velocity profile (Fig. 20) we obtain average jet velocity

$$v_{1m} = 4.32\sqrt{H_o} \text{ [m/s]}.$$

Since jet width downstream from the nozzle fluctuated between 115 and 117 mm, the following quantity of water, referred to 1 cm jet width, is obtained after nozzle calibration:

$$q = 0.827\sqrt{H_o} \text{ [l/s]}.$$

Thus the theoretical jet pressure per cm jet width, from (24), becomes /262

$$P_o = 0.365 H_o \sin\alpha_o.$$

This value is 4% too high relative to the measured value; the deviation can only be explained by an error in P_o in the calculation of jet velocity or quantity of water.

2. Trials with Round Jet

a) Nozzle Calibration

In order to determine jet velocity at the nozzle outlet, maximum velocity head H_o was measured as stagnation pressure at $\alpha_o = 90°$ for the nozzle without needle, as a function of pressure drop H'. The quantity of water was calibrated by means of tank measurements as for the rectangular jet. /263

b) Evaluation of Pressure Measurements

The pressure measurements were conducted at a total pressure upstream from the nozzle of H' = 20.46 m for the same panel positions as in the case of a rectangular jet. The pressure curve was measured in eight planes for each panel setting. Fig. 22 shows the evaluation of these trials for a panel inclination of 60°. We obtain the stagnation point and stagnation pressure, as well as jet pressure and its point of application, as the results. The theoretical location of flow lines in the impinging jet was determined on the basis of (32). If we transfer the measured stagnation pressures to these flow lines, we obtain a velocity distribution in the free jet which agrees with the measurements made by Thomann [4, 5].

c) Evaluation of Force Measurements

The diameter of the panel was about 3.2d (d = jet diameter). When the limits of error are taken into consideration, jet pressure can be balanced with a straight line $P = 48.5\sin\alpha_o$ for all panel angles with the pressure drop studied and thus follows the linear $\sin\alpha_o$ law.

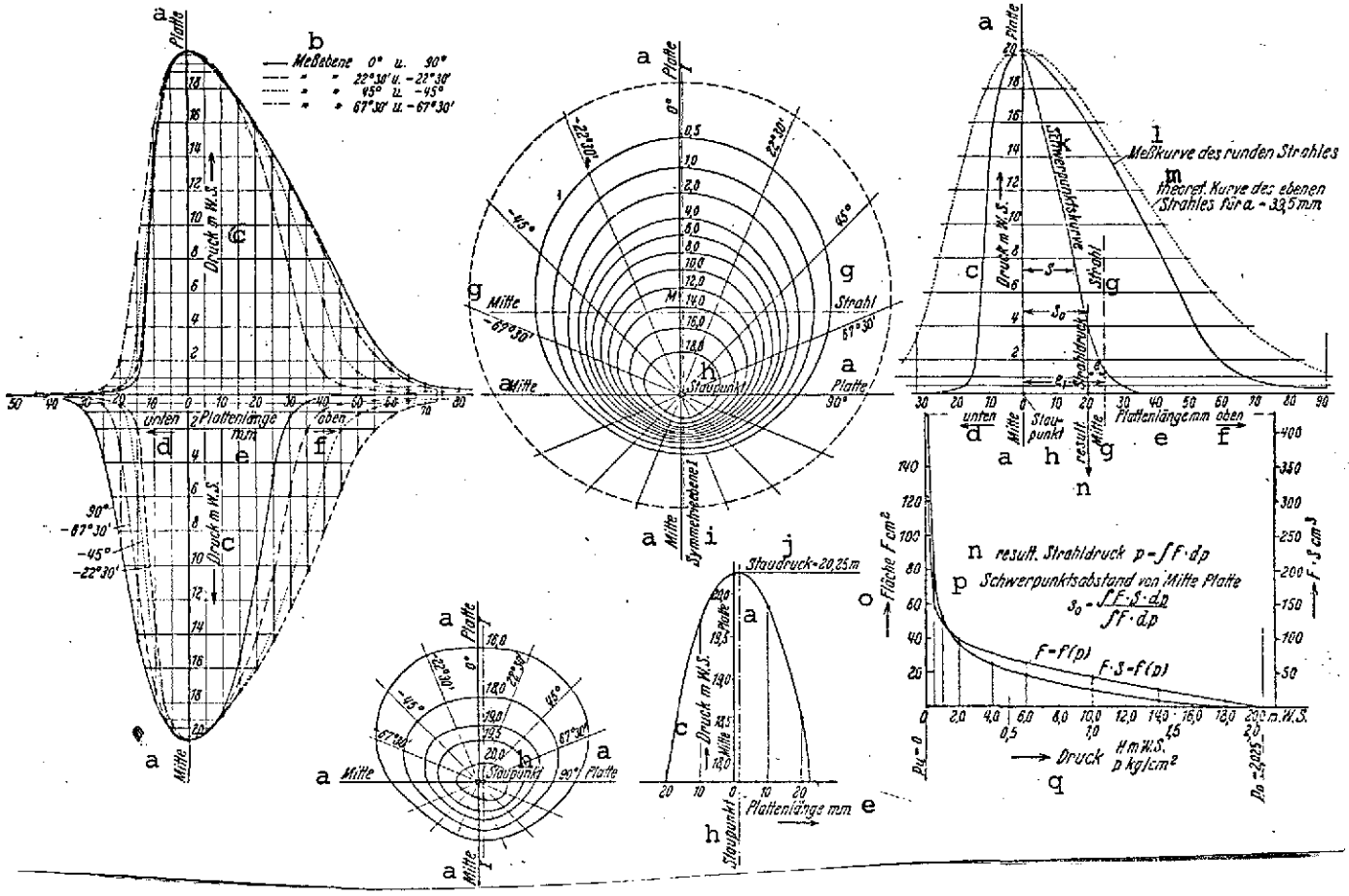

Fig. 22. Measurement of pressure at the panel for $\alpha_o = 60°$.

Key: a. Center of panel; b. Plane of measurements [u. = and]; c. Pressure in m H_2O; d. Down; e. Panel length in mm; f. Up; g. Center of jet; h. Stagnation point; i. Plane of symmetry; j. Stagnation pressure; k. Center of gravity curve; l. Measured curve for round jet; m. Theoretical curve for planar jet for a = 39.5 mm; n. Resultant jet pressure [F = area]; o. Area; p. Distance of center of gravity from center of panel; q. Pressure; W.S. = column of water

d) Calculation of Theoretical Jet Pressure

For a total pressure of H' = 20.46 m upstream from the nozzle, water throughput is Q = 24.4 ℓ/s, and the maximum velocity head of the jet is H_o = 20.35 m/s. On the basis of Thomann [4], we obtain an average jet velocity of v_{1m} = 19.68 to 19.78 m/s from this value H_o. We thus calculate theoretical jet pressure from Eq. (35) to be

$$P_o = (48.8 \text{ to } 49.5)\sin\alpha_o;$$

the measured jet pressure is from 0.5 to 2% too small relative to this value.

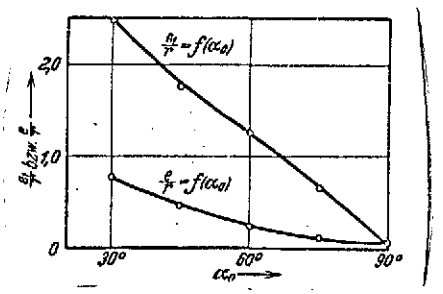

Fig. 23. Distance of stagnation point and point of jet pressure application from center of jet.

Key: bzw. = or

e) Determination of the Quantities of Water Flowing Off to Both Sides

The nozzle was adjusted in such a manner that the stagnation point fell on the horizontal line connecting the cutoff points, it being assumed that the filaments of water deflected exactly horizontally at the stagnation point coincide with the imaginary dividing line. As the paint trials showed, this is no longer the case at small angles α_o; however, shifting the nozzle from this center position reduced the error in the determination of water flow to only 1%. The experimental values are compared in Table 2 with the theoretical values calculated from Eq. (33).

IV. Summary

The theoretical treatment of a fluid jet which impinges obliquely upon a flat panel has been limited in the above to the

TABLE 2

Panel inclination	Measured values		Theoretical values (cf. p. 18)	
α_0	$\frac{Q_d}{Q}$	$\frac{Q_u}{Q}$	$\frac{Q_2}{Q}$	$\frac{Q_1}{Q}$
90°	0,511	0,489	0,50	0,50
75°	0,334	0,666	0,337	0,663
60°	0,181	0,819	0,195	0,805
45°	0,088	0,912	0,091	0,909
30°	0,027	0,974	0,029	0,971

[d = downward, u = upward]

deflection of a rectangular jet. For this planar problem, the free jet boundary and the distribtuion of flow within the jet are calculated with the aid of Prandtl's hodograph method, whereby the pressure distribution along the panel is also determined. The /264
calculation has been carried out for two examples, namely for perpendicular impingement and for an inclination of $\alpha_0 = 45°$. The free jet boundary and the pressure distribution along the panel can be determined with a small amount of computational work for any angle α_0. From this we obtain the characteristic values for flow (stagnation line and distance of stagnation point from center of jet, distribution of the quantities of water in the off-flowing jet, jet pressure and its point of application); these have been plotted in Fig. 10 for several angles α_0. The determination of flow lines within the jet requires a considerable amount of computational work, however, but they can be ascertained graphically or experimentally by one of the conventional methods, since the jet boundaries are known.

For the purpose of comparing these theoretical studies with actual flow, the pressure distribution over the panel has been determined experimentally for various panel inclinations, and perpendicular jet pressure and its point of application have been

calculated by integration of the pressure curves. Jet pressure was also determined directly by weighing in order to check the exerpimental results. Except for a few small deviations, the experimental pressure curves yield very good agreement with potential theory (cf. Fig. 19). Pressure measurements for various pressure drops and constant angle α_o produce the expected result that for constant jet thickness, pressure distribution along the panel and jet pressure vary as the square of jet velocity. The theoretical "law" of linear dependence upon the sine of inclination angle likewise applies to the variation in jet pressure with inclination α_o. The magnitude of jet pressure can be calculated from the equation

$$P_0 = \frac{q\gamma}{g} v_{1m} \sin \alpha_0$$

A difference of 4% was found between the theoretical and measured values; this must be attributed to an erroneous assumption in the determination of theoretical jet pressure from the nozzle calibration.

In order to study the deflection of a free fluid jet of circular cross section at a flat panel, we experimentally determined pressure distribution over the panel at the same panel inclinations as for the planar jet. From these pressure measurements we calculate the stagnation point and stagnation pressure, as well as jet pressure perpendicular to the panel and its point of application. Jet pressure was also measured directly by weighing to check the pressure measurements and the "laws" concerning jet pressure. It is found that, as in the case of the planar jet, jet pressure varies as the square of velocity and is a linear function of the sine of the angle of inclination. Measured jet pressure agrees with the theoretical value

$$P_0 = \frac{Q\gamma}{g} v_{1m} \sin \alpha_0$$

except for a deviation of 0.5 to 2%.

A cylinder having the stagnation line as its axis and elements perpendicular to the plane of symmetry divides the water throughput into two parts of different size. These components of water throughput have been calculated theoretically and also measured, yielding good agreement.

REFERENCES

1. Betz, A., and Petersohn, Ing.-Arch. 2, 190 (1931).

2. Trefftz, E., "The contraction of circular fluid jets," Dissertation, Strassburg, 1914.

3. Reich, "Deflection of a free fluid jet at a flat panel perpendicular to the direction of flow," Dissertation, Hannover, 1926.

4. Thomann, Die Wasserturbinen und Turbinenpumpen, [Water Turbines and Turbine Pumps], Part 2, Stuttgart, 1931.

5. Thomann, "Experiments on nozzles for free jet turbines with natural pressure drops," Escher Wyss Mitt., 1928.

6. Camerer, Vorlesungen über Wasserkraftmaschinen, [Lectures on Water Power Machines], 2nd edition, Leipzig, 1924.

7. Kaufmann, Angewandte Hydromechanik, [Applied Hydromechanics], Vol. 1, Berlin, 1931.

8. Handbuch der Physik, [Handbook of Physics], Vol. 7, Berlin, 1927.

9. Handbuch der Experimentalphysik, [Handbook of Experimental Physics], Vol. 4, Part 1: "Hydro- and Aerodynamics," Leipzig, 1931.

10. Wittenbauer, Z. Math. Physik 46, 182 (1901).

11. Nikuradse, "Principles of turbulent flow in smooth pipes," VDI-Forschungsh. 356 (1932).

12. Oesterlen, VDI Z. 70, 1215 (1926).